Prepared for submission to JHEP

Excited oscillons and charge-swapping

A. Alonso-Izquierdo[a,b] **D. Canillas Martínez**[b] **T. Romańczukiewicz**[c] **K. Sławińska**[c] **A. Wereszczyński**[c,d]

[a] *Departamento de Matemática Aplicada, University of Salamanca, Casas del Parque 2, 37008 - Salamanca, Spain*

[b] *IUFFyM, University of Salamanca, Plaza de la Merced 1, 37008 - Salamanca, Spain*

[c] *Faculty of Theoretical Physics, Astronomy and Applied Computer Science, Jagiellonian University, Kraków, Poland*

[d] *International Institute for Sustainability with Knotted Chiral Meta Matter (WPI-SKCM2), Higashi-Hiroshima, Hiroshima 739-8526, Japan*

E-mail: alonsoiz@usal.es, dnl.canillas@usal.es, tomasz.romanczukiewicz@uj.edu.pl, katarzyna.slawinska@uj.edu.pl, andrzej.wereszczynski@uj.edu.pl

Abstract: We show that the charge-swapping phenomenon can be understood as a real valued oscillon carrying an excitation in imaginary direction in the target space. Furthermore, we introduce a two dimensional collective model which quantitatively captures the charge swapping dynamics.

Contents

1 Introduction

Q-balls are non-topological solitons, that are localized, particle-like, nonperturbative solutions, which carry a $U(1)$ Noether charge [1, 2]. This charge arises from the global phase invariance of the action and therefore requires at least a complex field ϕ. In contrast to a topological charge, this charge is not quantized.

There are many areas of physics where Q-balls found an application. In cosmology, they are expected to be produced in the evolution of the early universe. In addition, they are considered as candidates for dark matter [3–6]. After coupling with gravity, they also give rise to boson stars [7, 8], i.e., hypothetical compact objects, whose imprint on gravitational wave measurements is now of great interest; see [9] for a review. The Q-balls can also be realized in condensed matter systems [10], e.g., in a superfluid [11].

The simplest Q-ball is a stationary solution, rotating in the complex target space with a constant frequency. Their properties, stability, and structure of small perturbations are quite well understood. If placed together, Q-balls begin to interact [12–14]. In some cases, this leads to the so-called *charge-swapping* phenomenon [15]. This is a quasi-stable solution in which the $U(1)$ charge periodically flows between two or more spatial regions.

Typically, charge-swapping solutions are found from an initial condition representing a pair of separated Q-ball and anti-Q-ball [15, 16]. This led to an interpretation of the charge-swapping phenomenon as a QQ^* bound state, where the constituent solitons form a kind of molecule [17]. More complicated examples, arising from a larger number of initial QQ^* pairs, were also presented.

In the current work, we present arguments that such an interpretation is not valid. Surprisingly, despite the fact that it can be generated from QQ^* initial data, the charge-swapping solution should be treated as an *excited oscillon*. (Concretely, this is an oscillon perturbed along the perpendicular direction in the target space.) This is another type of localized non-perturbative objects, whose stability does not rely on any topological or non-topological charge but is an effect of nonlinear self-interaction [18–20]. In fact, ocillons are not ultimately stable objects. All the time, they lose energy through radiation [21, 22] and eventually decay to vacuum. Nevertheless, the life-time of an oscillon can be extremely long [23–27], sometimes comparable to the age of the universe, which makes them important in the dynamics of various solitons. Similarly to Q-balls they have various cosmological and astrophysical applications, for example [28–32].

The main support for our conclusion is found in the mode structure of the charge-swapping states, which is clearly inherited from the oscillon, not from the Q-balls. Furthermore, charge-swapping solutions are generated from much more general initial data, which represent such a perturbed oscillon rather than only a QQ^* pair.

2 The complex ϕ^6 model

2.1 The Q-balls

In this work we will focus on the simplest Q-ball theory which is the complex ϕ^6 model in (1+1) dimensions

$$\mathcal{L} = \partial_\mu \phi \partial^\mu \phi^* - |\phi|^2 - |\phi|^4 + \beta |\phi|^6 \,. \tag{2.1}$$

The equations of motion are

$$\phi_{tt} - \phi_{xx} + (1 + 2|\phi|^2 - 3\beta|\phi|^4)\phi = 0 \tag{2.2}$$

and the complex conjugation. Due to the global $U(1)$ symmetry, $\phi \to e^{i\lambda}\phi$, there is a conserved current j^μ and conserved Noether charge Q

$$j_\mu = i\left(\phi^* \partial_\mu \phi - \phi \partial_\mu \phi^*\right), \quad Q = \int_{-\infty}^{\infty} \rho \, dx. \tag{2.3}$$

Here $j^0 \equiv \rho$. The simplest, single Q-ball solution is a stationary configuration rotating in the target space with the frequency ω_0

$$\phi = f_{\omega_0}(x) e^{i\omega_0 t}, \tag{2.4}$$

which profile $f_{\omega_0}(x)$ reads

$$f_{\omega_0}(x) = \frac{\sqrt{2}\epsilon}{\sqrt{1 + \sqrt{1 - 4\beta\epsilon^2}\cosh(2\epsilon x)}} \,. \tag{2.5}$$

Here, $\epsilon = \sqrt{1 - \omega_0^2}$. The Q-ball carries the following energy and the $U(1)$ charge

$$E(\omega_0) = \frac{4\omega_0\epsilon + Q(4\beta - 1 + 4\beta\omega_0^2)}{8\omega_0\beta}, \quad Q(\omega_0) = \frac{4\omega_0}{\sqrt{\beta}} \operatorname{arctanh}\left(\frac{1 - \sqrt{1 - 4\beta\epsilon^2}}{2\epsilon\sqrt{\beta}}\right) . \tag{2.6}$$

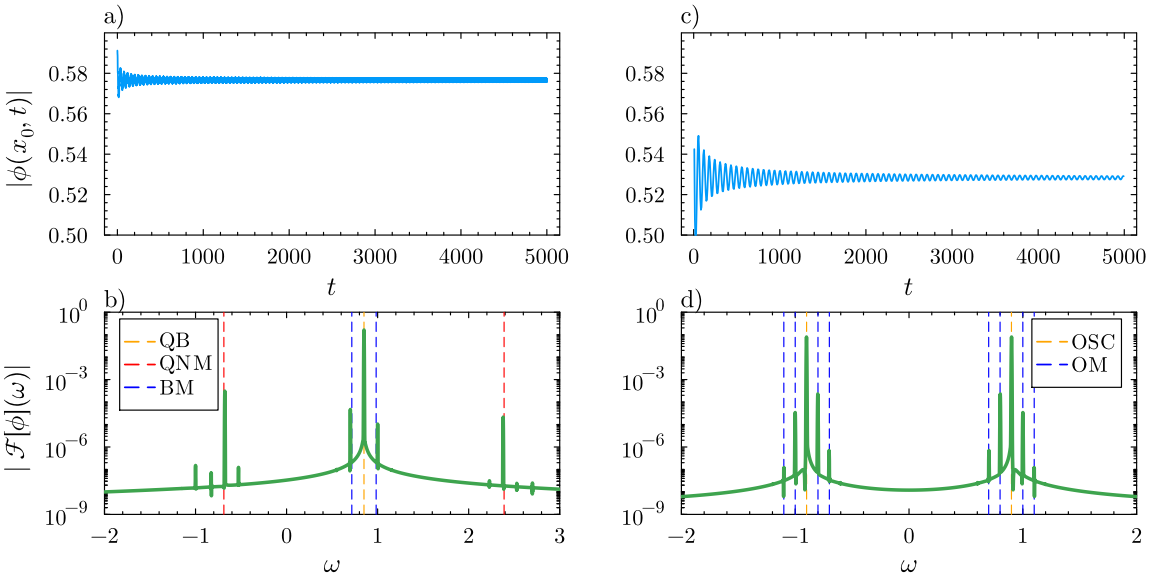

Figure 1. Time dependence of the maximum of Re ϕ and the power spectrum of a perturbed Q-ball with $\omega_0 = 0.85$ and $\lambda = 1.05$ (left) and oscillon (right). Here $\beta = 0.5$.

Although the Q-balls exist for $\omega_0 \in [\omega_{min}, \omega_{max}]$, where $\omega_{min}^2 = 1 - \frac{1}{4\beta}$ and $\omega_{max} = 1$, they are classically stable only if

$$\frac{\omega_0}{Q}\frac{dQ}{d\omega_0} < 0. \tag{2.7}$$

It has been recently noticed that Q-balls possess quite a rich structure of linear modes [33]

$$\delta\phi(x,t) = \eta_1(x)e^{i(\omega_0+\rho)t} + \eta_2(x)e^{i(\omega_0-\rho)t}. \tag{2.8}$$

Note that a mode has two components $\eta_{1,2}$ with frequencies $\omega_0 \pm \rho$. Therefore, for stable Q-balls, three possibilities can be identified. There can be a bound mode (BM) if the frequencies of both components are below the mass threshold. If one frequency is above the mass threshold, we have a quasinormal mode (QNM) known as the Feshbach resonance. In this case, one component of the mode is still bounded to the Q-ball. If both frequencies are above the mass threshold, we get a genuine scattering mode. Of course, there are also zero modes that reflect translational and $U(1)$ symmetries. In the unstable regime, an unstable mode additionally appears.

In Fig. 1, left panels, we display the mode structure of a perturbed Q-ball. Specifically, we take $\beta = 0.5$ and $\omega_0 = 0.85$. Perturbation is provided by a radial squeeze by factor $\lambda = 1.05$. In the spectrum, there is the main frequency (QB) at ω_0, a bound mode (BM) with $\rho = 0.133612$ and a quasinormal mode (QNM) with $\rho = 1.538789 + 1.18 \cdot 10^{-5}i$, highlighted respectively by orange, blue and red dashed lines.

2.2 The Oscillons

The (complex) ϕ^6 model, as many models with nonlinear self-interaction, supports oscillons, i.e., approximately periodic in time, localized field configurations. Recently, it has been

shown that the oscillon and Q balls are, in fact, very closely related to each other [34]. Especially in the ϕ^6 theory, these objects are somehow dual to each other [35]. An oscillon can be viewed as formed from two opposite charge Q-balls or, vice versa, a Q-ball can be treated as a bound state of two oscillons, each in each real and imaginary component of the complex field [15, 35]. In addition, also their mode structures are related [35].

In Fig. 1, right panel, we show an example of the oscillon generated from the initial profile $\phi(x,0) = \frac{2}{\sqrt{3}}\frac{\epsilon}{\cosh(\epsilon x)}$. The spectrum is $\mathbb{Z}_2$ symmetric. The main peak at ω_O corresponds to the fundamental frequency of the oscillon (OSC). The other peaks at $\omega_O \pm n\omega_{mod}$ (OM) can be interpreted as an effect of the appearance of another small-amplitude oscillon. Importantly, ω_{mod} is the frequency of the amplitude modulation. Here, $\omega_O = 0.90$ and $\omega_{mod} = 0.10$.

3 Charge-swapping

3.1 Charge-swapping from QQ^* Initial Conditions

A charge-swapping solution is typically generated from the initial state being a separated pair of the Q-ball and anti-Q-ball [15, 16]

$$\Phi(x,t) = f_{\omega_0}(x+x_0)e^{i\omega_0 t} + f_{\omega_0}(x-x_0)e^{-i\omega_0 t}. \tag{3.1}$$

Depending on the separation $d = 2x_0$ this configuration relaxes to two excited Q-balls or to a charge swapping state.

In Fig. 2 we present examples of dynamics generated from the initial data (3.1). Here we fix $\beta = 0.5$ and $\omega_0 = 0.85$. We plot the time evolution of the charge density as well as the real and imaginary components of the complex field. In the upper panels, we show the case where the Q-balls remain independent. In the middle panel, there is a single-bounce solution, while in the bottom panel, there is a dynamics with charge swapping.

In general, we may identify three regimes. If the initial separation is large enough, $x_0 > \tilde{x}$, the force between the Q balls is weak, and they remain independent throughout the simulation, which in our case ends at $t_{max} = 500$. For smaller separations, $\tilde{x} > x_0 > x_{cr}$ the attraction becomes stronger, and Q-balls collide. They bounce once and separate or enter into a rather irregular, chaotic multi-bounce regime. It is clearly seen that after the first collision the bouncing Q-balls vibrate. Eventually, for even smaller initial separation, $x_0 < x_{cr}$, the QQ^* initial data form a well-visible and quite stable charge-swapping solution. The critical value x_{cr} depends on the model parameter β and the parameter ω_0 of the initial state. On the other hand, $\tilde{x}$ is not a universal quantity. For the growing time of the simulation $\tilde{x}$ also increases. This is because there is always an attractive force between the Q-ball and the anti-Q-ball. Hence, eventually the solitons will always collide.

In Fig. 3, upper panel, we present the dependence of the final state of the evolution on the value of the parameter x_0 in the initial configuration. We clearly see the three regimes mentioned above. Concretely, we plot the charge distribution at $t_{max} = 300$ for $\beta = 0.5$ and $\omega_0 = 0.85$. The critical value of the parameter x_0 is $x_{cr} = 2.87(2)$ while $\tilde{x} \approx 6.1$. Interestingly, the multi-bounce regime reveals a self-similar pattern which

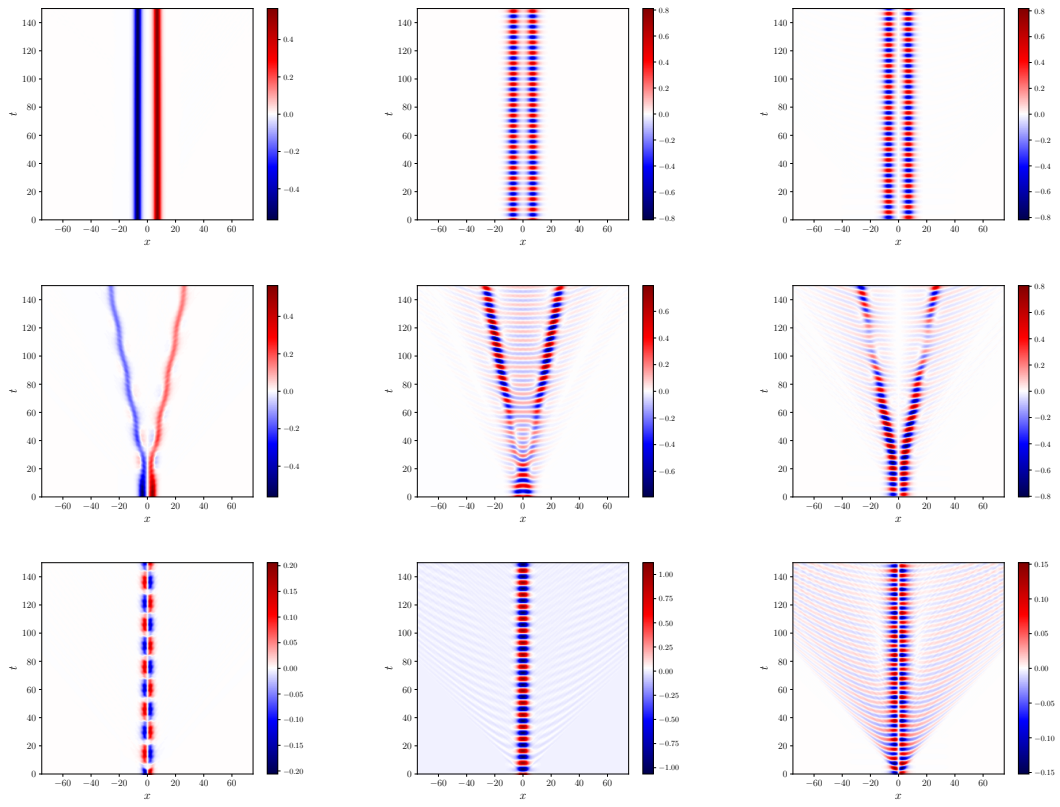

Figure 2. Examples of time evolution obtained from Q-ball-anti-Q-ball initial data (3.1). Here $\beta = 0.5$ and $\omega_0 = 0.85$ while $x_0 = 7.5$ (upper row), $x_0 = 3.5$ (middle row) and $x_0 = 0.5$ (lower row). We plot: the charge density (left column), Re (ϕ) (middle column) and Im (ϕ) (right column).

suggests chaotic behaviour, see Fig. 3 lower panel, where we zoom on the previous plot. This fractal structure occurs in various solitonic processes, such as, for example, kink-antikink scatterings [36–38] (also [39–41]), collisions of vortices [42, 43] or oscillon decay [44], and is triggered by the resonance transfer mechanism. Furthermore, in this plot, we also show how the difference between the charges stored in $x > 0$ and $x < 0$ evolves in time, $\Delta Q = Q(x < 0) - Q(x > 0)$, where $Q(x < 0)$ is the charge in half space with $x < 0$.

It is important to note that although for $x_0 \to 0$ we always see charge swapping, the amount of charge that actually is exchanged is decreasing to zero. Similarly, the imaginary component of the complex field is also less excited as the separation parameter in the initial configuration tends to 0. Eventually, in the limit $x_0 \to 0$ we find an excited (modulated) oscillon which has zero charge density. Of course, this is a consequence of the form of the initial configuration. As x_0 approaches zero it is just

$$\Phi(x,t) = 2f_{\omega_0}(x)\cos(\omega_0 t) + 2ix_0 f'_{\omega_0}(x)\sin(\omega_0 t). \tag{3.2}$$

Exactly for $x_0 = 0$ only the real component of the field is excited. Then, the initial configuration, $\Phi(x,t) = 2f_{\omega_0}(x)\cos(\omega_0 t)$, relaxes to a real oscillon with an even perturbation.

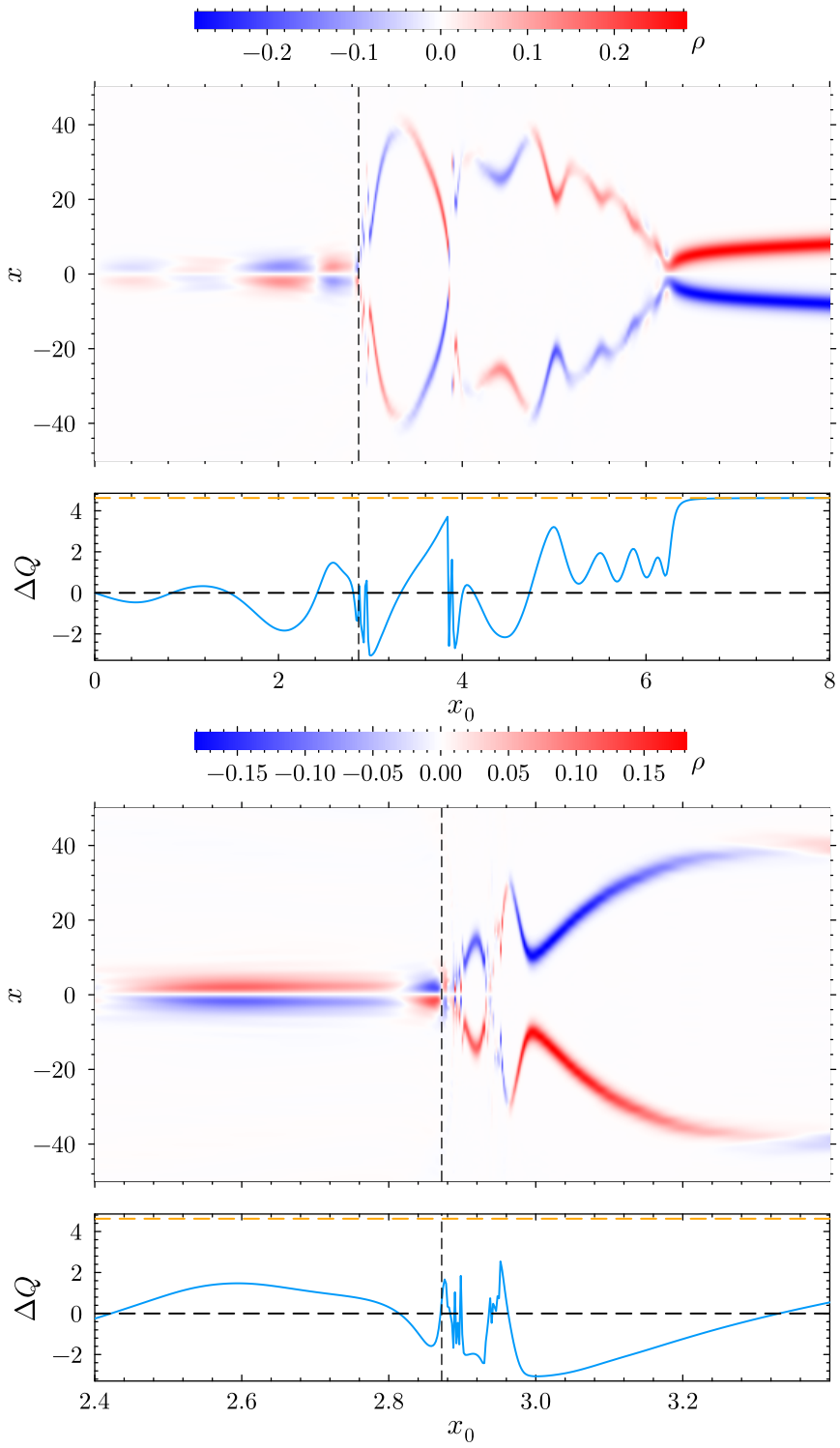

Figure 3. The charge density at $t_{max} = 300$ as a function of parameter x_0. The vertical line at $x_{cr} = 2.87(2)$ separates the charge-swapping regime from other scenarios: the multi-bounce solutions and separated Q-balls. Here $\Delta Q = Q(x < 0) - Q(x > 0)$.

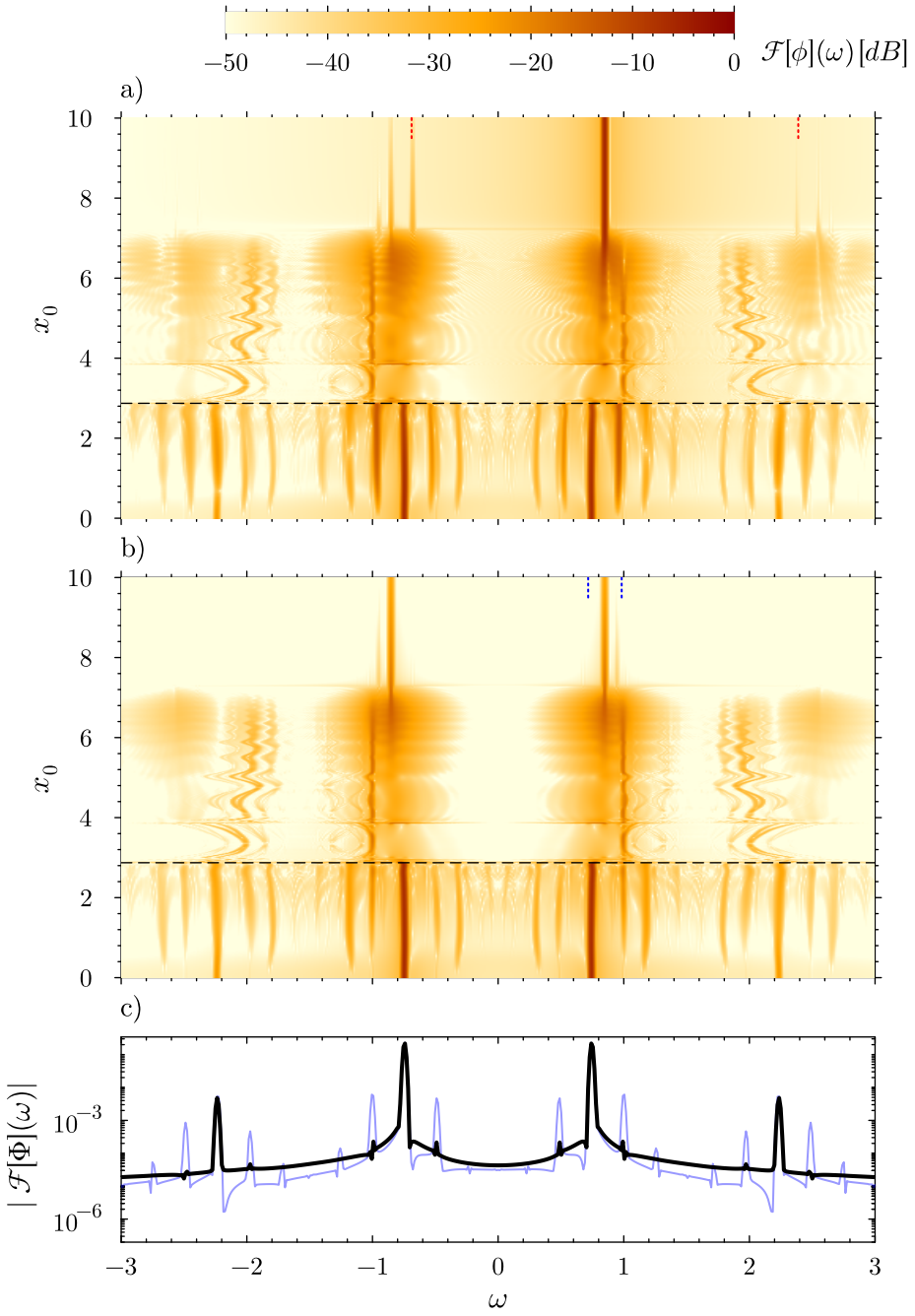

Figure 4. Power spectrum at $x = x_0$ (upper panel) and $x = 0$ (lower panel) for the solution found from the QQ^* initial configuration (3.1). Here $\beta = 0.5$, $\omega_0 = 0.85$ and time of the evolution is $t_{max} = 500$. At the bottom the power spectrum of the oscillon (blue) and an excited oscillon (black). Horizontal dashed line denotes $x_{cr} = 2.87(2)$.

A small x_0 provides an additional odd perturbation of the oscillon along the imaginary component of the field.

In order to better understand the change-swapping solutions, we show the dependence of the power spectrum, computed for the solution generated from the initial data, on the

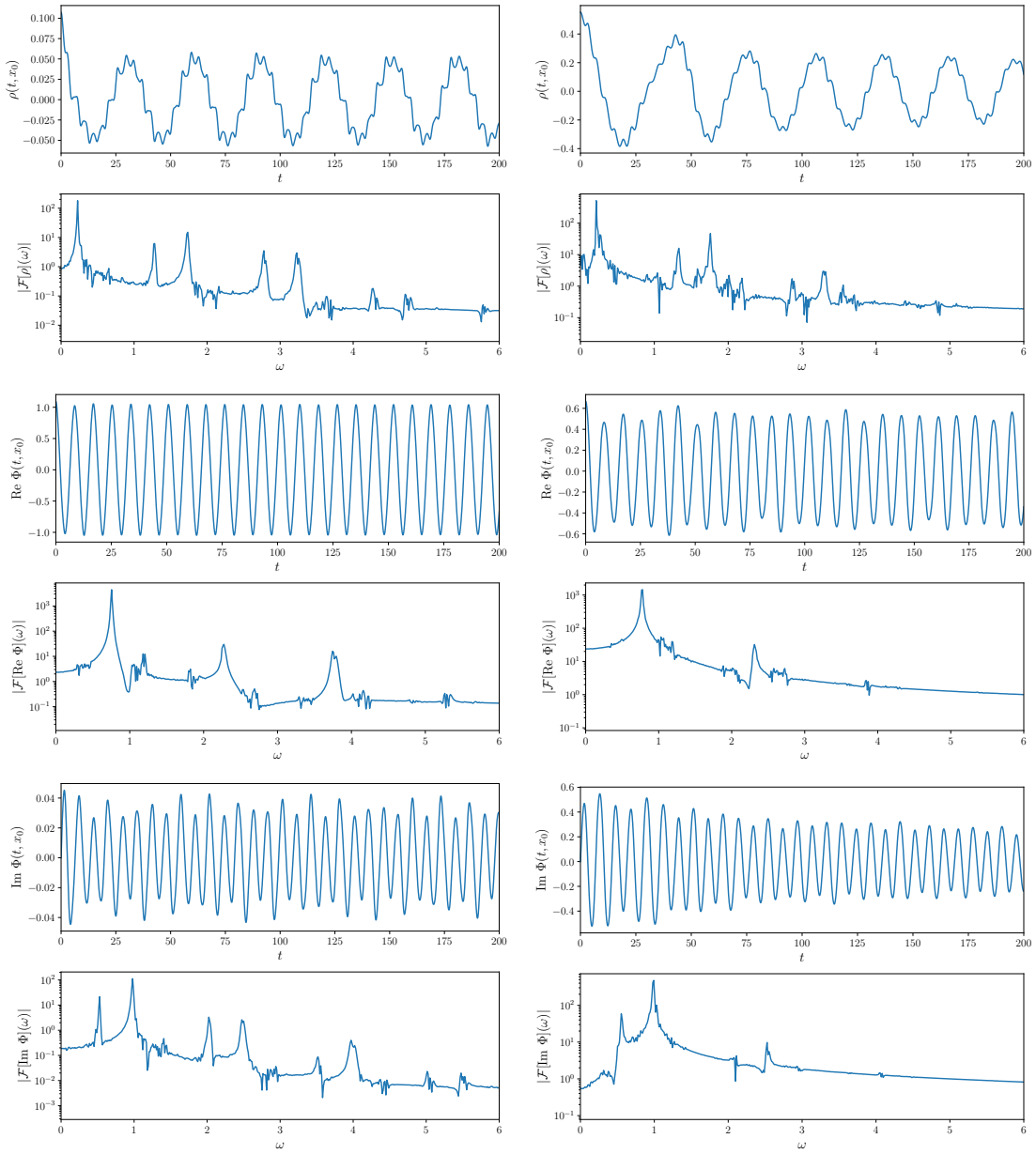

Figure 5. Example of the charge swapping solution obtained from the QQ^* initial data (3.1) with $x_0 = 0.5$ (left) and $x_0 = 2.5$ (right). Here $\beta = 0.5$ and $\omega_0 = 0.85$. We plot charge density ρ, Re ϕ and Im ϕ at $x = x_0$ as well as the corresponding power spectra.

separation parameter x_0, see Fig. 4. This plot further confirms the existence of the three regimes. First of all, for large separation, $x_0 > 7.2$, the Q-ball do not have time to collide ($t_{max} = 500$). Consequently, the power spectrum reveals the typical structure of an excited Q ball, where the excitation comes from the presence of the second Q ball. In fact, there are two main peaks: one at the internal frequency $\omega = \omega_0$ and another one corresponding to the quasinormal mode (red dashed line). For smaller separations, $7.2 < x_0 < 2.9$, the Q-balls collide. The irregular multi-bounce regime is visible as a diffuse region in the power

spectrum where the peak related to the internal frequency ω_0 rapidly widens and gradually disappears from the spectrum.

Finally, for $x_0 < 2.9$, the initial configuration relaxes to the proper charge-swapping solution. Surprisingly, *the mode spectrum is not inherited from the Q-balls but from the excited oscillon*, realized at $x_0 = 0$. The spectrum is $\mathbb{Z}_2$ symmetric, a characteristic feature of an oscillon, with the leading peak at the fundamental oscillon frequency $\omega_O = 0.7540$. This frequency changes very little over the whole charge swapping regime. There are additional peaks which also move slightly while we change x_0. The peaks can be easily explained by analyzing the power spectrum of the real and imaginary parts of the field separately, see Fig. 5.

The fundamental frequency is visible as the main peak in the spectrum of the real component. This is due to the fact that at $x_0 = 0$ we find the real-valued oscillon. It changes from $\omega_{\rm Re} = 0.7540$ at $x_0 = 0.5$ to $\omega_{\rm Re} = 0.7791$ at $x_0 = 2.5$, which is close to the end of the charge-swapping regime. This frequency is absent in the spectrum of the imaginary part. Here, the main peak is located just below the mass threshold, that is, $\omega_{\rm Im} = 0.9801$ for $x_0 = 0.5$ and $\omega_{\rm Im} = 0.9927$. As originally observed in [16], these two frequencies trigger charge swapping. Its frequency is simply $\omega_{CS} = \omega_{\rm Im} - \omega_O$ and is seen as the main peak in the power spectrum of the charge density at $\omega_{CS} = 0.2262$ for $x_0 = 0.5$ and at $\omega_{CS} = 0.2136$ for $x_0 = 2.5$. The second main peak corresponds to $\omega_O + \omega_{\rm Im}$.

3.2 Charge-swapping from Generic Perturbed Oscillon Initial Conditions

The small x_0 expansion also suggests that a charge-swapping solution can be generated if we start with a generic imaginary-valued perturbation of the real oscillon, not necessarily related to the split QQ^* configuration. In fact, we found charge-swapping considering a general complex-valued perturbation of the oscillon in the real component of the complex field

$$\phi(x,0) = \phi(x) + A_r g_1(x), \quad \partial_t \phi(x,0) = i\omega A_i g_2(x), \tag{3.3}$$

where $\phi(x) = \frac{2}{\sqrt{3}} \frac{\epsilon}{\cosh(\epsilon x)}$ is an approximated profile of the oscillon while the perturbation profiles are

$$g_1(x) = \frac{1}{\cosh(\epsilon x/4)}, \quad g_2(x) = \frac{\tanh(\epsilon x/4)}{\cosh(\epsilon x/4)}. \tag{3.4}$$

$A_{r,i}$ are the amplitudes of the perturbations in the real and imaginary component. We assume that the perturbation is wider than the original profile of the oscillon.

For $A_r \neq 0$ and $A_i = 0$ we obtain a standard perturbed real oscillon with some characteristic amplitude modulation. There is no excitation in the imaginary part of the complex field. Thus, the charge density vanishes identically.

On the other hand, if we excite the imaginary component of the field, then charge density has a non-trivial distribution, even though the total charge is still zero. What is more important, these initial data amounts to the charge-swapping phenomenon. Again, the initial perturbation excites some oscillations in the imaginary part of the field with a frequency different from the frequency of the perturbed real-component oscillon. This difference leads to charge oscillations. However, generically, not the full charge is swapped

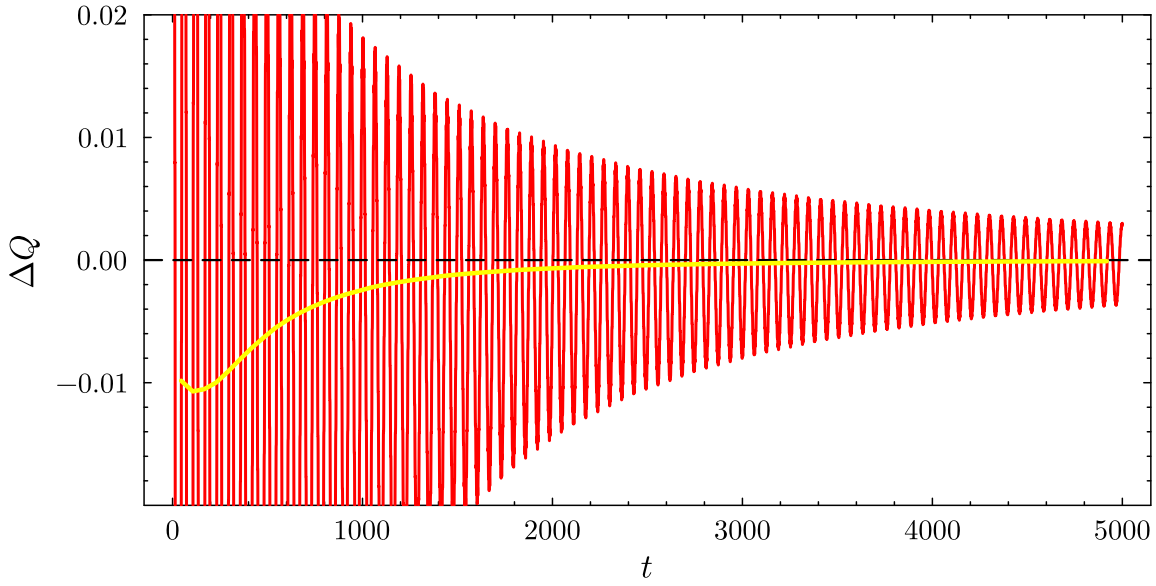

Figure 6. Time evolution of charge stored in the half-plane $x > 0$ for the perturbed oscillon initial conditions (3.3) with $A_r = 0$ and $A_i = 0.1$. Yellow curve denotes the average charge around which the charge oscillates.

between the $x > 0$ and $x < 0$ regions. This is clearly seen in Fig. 6 where we show the time dependence of ΔQ. This charge oscillates around a negative value, which asymptotically tends to 0 recovering the usual full charge-swapping. We remark that one can fine-tune the initial data to obtain the full charge-swapping from the very beginning.

In Fig. 7 we present the power spectra of solutions obtained from the perturbed oscillon. As expected for the oscillon, the spectrum consists of a set of equally separated peaks, which reveals a $\mathbb{Z}_2$ symmetry. This should be contrasted with the spectrum of a perturbed Q-ball (squeezing by the factor $\lambda = 1.05$), see the bottom panel.

All this proves that the charge-swapping phenomenon is the result of a perturbation of the oscillon in the perpendicular direction (in the sense of the target space) rather than a QQ^* bound state.

4 The collective coordinate model

To obtain a collective description of the charge-swapping we need to have a set of configurations that occur in this phenomenon, at least approximately. Therefore, a natural choice would be to take an approximate oscillon perturbed in the imaginary direction, e.g. (3.3). From the above analysis, it is obvious that such configurations can also be achieved using a QQ^* superposition with appropriately rescaled profiles of the Q-balls. This induces two collective coordinates: the positions of the Q-balls, x_0, and their amplitude α. This has the advantage that it smoothly interpolates between a perturbed oscillon and a separated QQ^* pair, and therefore it might even cover the formation of the charge-swapping solution from colliding Q-balls. In addition, in the single Q-ball sector, the collective variables α

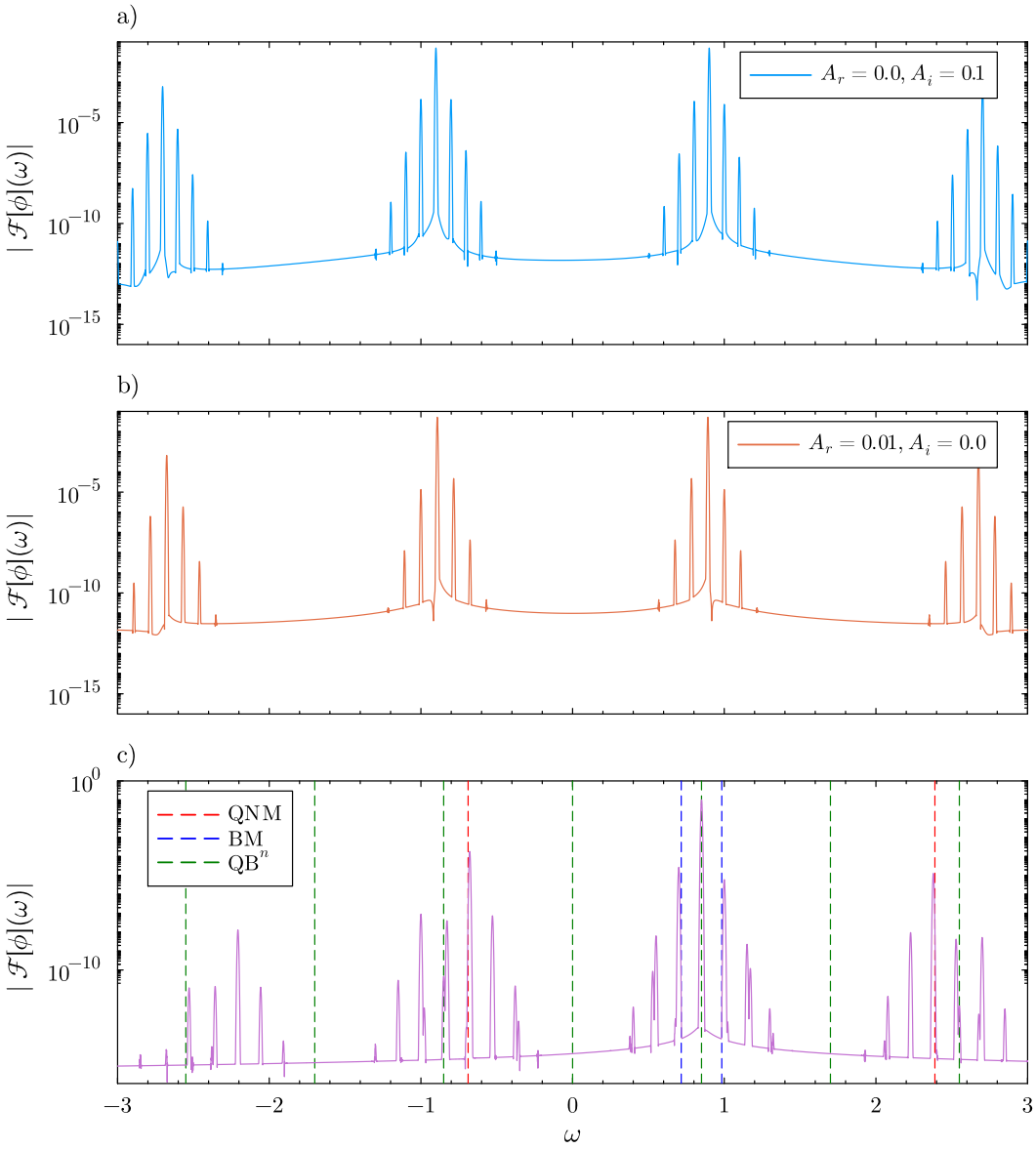

Figure 7. Power spectra of the the perturbed oscillon initial conditions (3.3) (upper and middle panels) compared with a perturbed Q-ball (bottom), where the quasi-normal mode (QNM), bound mode (BM) and fundamental Q-ball frequency are marked.

and θ describe the excitation of the Q-ball. They must be included simultaneously due to charge conservation [13].

All these motivate the following set of configurations

$$\Phi(x) = \alpha \left(f_\omega(x + x_0) e^{i\theta} + f_\omega(x - x_0) e^{-i\theta} \right), \tag{4.1}$$

where the collective coordinates (moduli) $(X^1, X^2, X^3) = (\alpha, \theta, x_0)$ will be promoted to time-dependent variables [45]. Furthermore, f_ω is the profile of the Q-ball with frequency ω. This choice defines the initial condition for the velocity of the coordinate θ. In the

CCM framework, the full dynamics will be approximated by the dynamics of the moduli. In general, this set leads to a three-dimensional collective coordinate model (CCM).

In the current paper, we will consider its two-dimensional version, where only $(X^1, X^2) = (\alpha, \theta)$ are dynamical variables, while $X^3 = x_0$ is treated as a fixed parameter. This greatly simplifies computations and still gives very accurate results. Thus, as the separation is kept constant, this version cannot describe the coalescence of the Q-ball with the anti-Q-ball. However, it is able to cover dynamics in each sector separately and predict at which separation the charge-swapping state shows up.

The Lagrangian of this CCM reads

$$L[\alpha, \theta] = g_{ij}\dot{X}^i\dot{X}^j - V(X^1, X^2), \tag{4.2}$$

where the moduli space metric is

$$g_{ij} = \begin{pmatrix} \frac{Q}{\omega} + 2\mathcal{I}\cos(2\theta) & -2\mathcal{I}\alpha\sin(2\theta) \\ -2\mathcal{I}\alpha\sin(2\theta) & \alpha^2\left(\frac{Q}{\omega} - 2\mathcal{I}\cos(2\theta)\right) \end{pmatrix}. \tag{4.3}$$

Here

$$\mathcal{I}(x_0) = \int_{-\infty}^{\infty} f_\omega(x + x_0) f_\omega(x - x_0) dx \tag{4.4}$$

measures the spatial overlap of the Q-ball and anti-Q-ball profiles. It is easy to show that $0 \leq \mathcal{I} \leq \frac{Q}{2\omega}$. For infinitely separated solitons, $x_0 \to \infty$, the overlap tends to 0. For the on-top configuration, that is, when $x_0 \to 0$, we get $\mathcal{I} = \frac{Q}{2\omega}$.

The effective potential V is a sixth order polynomial in α

$$V(\alpha, \theta) = \sum_{j=0}^{3}\sum_{k=1}^{3} C_k^{(j)} \alpha^{2k} \cos(2j\theta), \tag{4.5}$$

where $C_k^{(j)}$ are constants depending on x_0, which have to be computed numerically, see Appendix A.

The CCM gives a well-defined two-dimensional dynamical system for any $x_0 > 0$. However, exactly at $x_0 = 0$, where the positions of the Q balls coincide, we encounter a singularity. This can be seen in the determinant of the metric

$$\det g = \alpha^2\left(\frac{Q^2}{\omega^2} - 4\mathcal{I}^2\right) \tag{4.6}$$

which is identically zero for $x_0 = 0$. The reason for this is that the set of complex configurations (4.1) reduces to real functions at this point, effectively lowering the dimensionality of the moduli space for $x_0 = 0$. A consequence of this is an observation that the description of the oscillon within this CCM is highly simplified. Exactly at $x_0 = 0$, the CCM has only one dynamical coordinate. Thus, the oscillon is modeled in terms of a one-dimensional anharmonic oscillator. This obviously neglects several important features of the oscillons, e.g. modulation of the amplitudes, which requires at least two degrees of freedom [34, 46], see also [47, 48]. Nevertheless, for our purposes, it is enough to include the oscillon in such

a simplified way. Note that there is a second point at which the determinant of the metric vanishes, $\alpha = 0$. However, it is an apparent coordinate system singularity, identical to the singularity of the polar coordinates.

There exists another convenient set of collective coordinates that removes the apparent singularity. Namely, $(X^1, X^2) = (X, Y)$ being the Cartesian coordinates on the complex target space

$$X = \alpha \cos\theta, \quad Y = \alpha \sin\theta. \tag{4.7}$$

Then, the real and imaginary parts of the complex field are simply

$$\begin{aligned} \mathrm{Re}\,\phi(x,t) &= (f_\omega(x+x_0) + f_\omega(x-x_0))\, X(t), \\ \mathrm{Im}\,\phi(x,t) &= (f_\omega(x+x_0) - f_\omega(x-x_0))\, Y(t). \end{aligned} \tag{4.8}$$

Importantly, the corresponding metric is diagonal and constant

$$g_{ij} = \begin{pmatrix} \frac{Q}{\omega} + 2\mathcal{I} & 0 \\ 0 & \frac{Q}{\omega} - 2\mathcal{I} \end{pmatrix}. \tag{4.9}$$

This smooth change of variables cannot affect the existence of the singularity at $x_0 = 0$. In fact, in this limit the g_{YY} component of the metric is zero, which obviously leads to zero of the determinant. Since the metric is flat and diagonal, all the dynamics are encoded into the nonlinearities of the effective potential, which, written in the Cartesian coordinates, is an even polynomial of the sixth order and reads

$$\begin{aligned} V(X,Y) = {} & D_{2,0}X^2 + D_{4,0}X^4 + D_{6,0}X^6 + D_{0,2}Y^2 + D_{0,4}Y^4 + D_{0,6}Y^6 \\ & + D_{2,2}X^2Y^2 + D_{4,2}X^4Y^2 + D_{2,4}X^2Y^4. \end{aligned} \tag{4.10}$$

In Appendix A, we give integral expressions for these coefficients and their relation to the constants $C_k^{(j)}$. Qualitatively, the potential is simply a nonaxially symmetric anharmonic potential with only one minimum at $X = Y = 0$. In the limit of separated Q balls, when $x_0 \to \infty$, it recovers the axial symmetry as both Q balls independently rotate in the target space, although already for $x_0 \approx 3$ it has a quite symmetric shape, see Fig. 11 in Appendix A. In the limit where $x_0 \to 0$ the potential becomes more and more flattened in the Y direction. However, because the metric component g_{YY} also vanishes in this limit, all excitations in this direction are suppressed.

To reproduce the full field theory dynamics we apply the CCM with the following initial conditions

$$\alpha(0) = 1, \quad \dot\alpha(0) = 0 \tag{4.11}$$

$$\theta(0) = 0, \quad \dot\theta(0) = \omega, \tag{4.12}$$

that is

$$X(0) = 1, \quad \dot X(0) = 0 \tag{4.13}$$

$$Y(0) = 0, \quad \dot Y(0) = \omega, \tag{4.14}$$

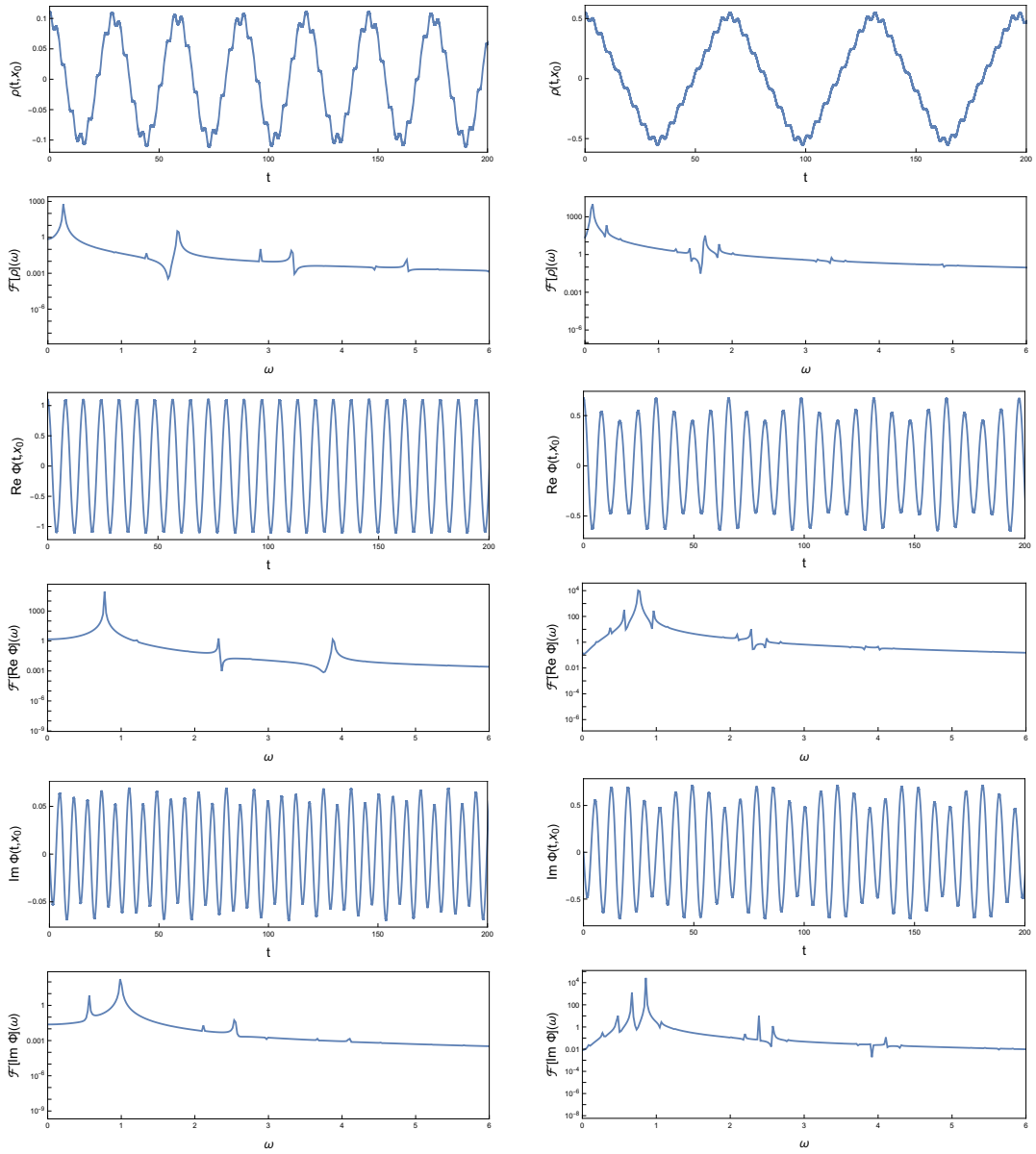

Figure 8. Charge-swapping solutions obtained from the CCM with $x_0 = 0.5$ (two upper rows) and $x_0 = 2.5$ (two lower rows). Here $\beta = 0.5$ and $\omega_0 = 0.85$. We plot charge density ρ, Re ϕ and Im ϕ at $x = x_0$ as well as the corresponding power spectra.

which coincide with the choice of the set of configuration (4.1). In Fig. 8 we present the dynamics obtained in the CCM (4.2) for $\beta = 0.5$ and $\omega_0 = 0.85$. Specifically, we chose $x_0 = 0.5$ and $x_0 = 2.5$ which corresponds to the initial data for the full field theory numerics shown in Fig. 5. We found good agreement, especially for the case with small x_0. The amplitudes of oscillations of the real and imaginary components of the field agree well with the full theory numerics although, generically, they are bigger. This is best visible in the amplitude of the charge-swapping. This is due to the fact that the initial configuration

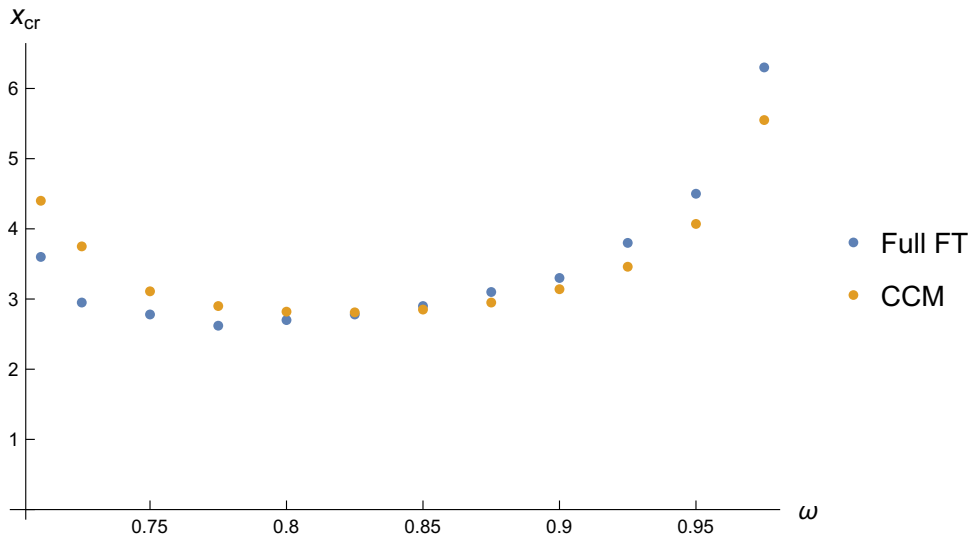

Figure 9. The dependence of the critical value of the parameter x_{cr} on the frequency ω of the initial QQ^* configuration. For $x_0 < x_{cr}$ we find the charge-swapping solution.

radiates quite a lot at the initial stage of the full field-theoretical evolution. This is, of course, not possible in the CCM since no radiative degrees of freedom are included. Hence, all the initial energy goes to the oscillating solutions.

Although the CCM predicts amplitudes of the field and charge density that are larger than those observed, it accurately reproduces the frequencies. That is, the fundamental frequency of the perturbed oscillon is $\omega_{\rm Re} = 0.7749$, for $x_0 = 0.5$ and $\omega_{\rm Re} = 0.7540$ for $x_0 = 2.5$, which are very close to the values found in the full field theory. The main frequency of the imaginary component is more sensitive to the value of x_0. For $x_0 = 0.5$, we get $\omega_{\rm Im} = 0.9840$, which is quite close to the true value. However, for $x_0 = 2.5$, the discrepancy is much larger, $\omega_{\rm Im} = 0.8587$. In any case, this leads to a good prediction of the charge-swapping frequency, especially in the small x_0 limit - $\omega_{CS} = 0.2095$ for $x_0 = 0.5$. For larger x_0, disagreement grows; for example, for $x_0 = 2.5$, we find $\omega_{CS} = 0.1047$.

Finally, our CCM can be used to predict for which x_0, that is, for which separation of the initial QQ^* pair, the charge-swapping state is formed. In Fig. 9 we compare the full field theory result with the CCM computation. The agreement is very good. Undoubtedly, such a simple CCM predicts the dependence of the critical distance x_{cr} on the initial frequency ω.

5 Summary

Since its discovery, the charge-swapping phenomenon has been treated as a bound state of Q-ball and anti-Q-ball. Despite the fact that it arises from such an initial state, we have clearly shown that it should rather be understood as an excited oscillon; that is, an oscillon with a charged wave. The main argument supporting this conclusion comes from the analysis of the mode structure of the charge-swapping solutions, which is basically the

same as the spectrum of the oscillon. In addition, the charge-swapping solution is easily formed from perturbed oscillon initial data, where the perturbation is along the imaginary direction.

In addition, we constructed a collective coordinate model (CCM) that captures the essence of the charge-swapping mechanism. Even in the simplest two-dimensional version, it is able to model the charge-swapping solutions with reasonably good accuracy. It predicts the frequencies of the field oscillations as well as the charge-swapping frequency, especially well in the limit of small imaginary perturbation of the real oscillon, that is, in the small x_0 limit. We expect that the three-dimensional CCM, where the parameter x_0 becomes a dynamical variable, will significantly improve the collective description. However, this requires a careful treatment of the singularity in $x_0 = 0$. A natural approach to this issue can be based on the perturbative relativistic moduli space framework developed in [49] and successfully applied to kink-antikink collisions.

In our analysis, we also found evidence that the interaction of the Q-balls reveals a chaotic pattern, very similar to collisions of domain walls (kinks) [36–38] and local vortices [42, 43]. Similarly as in the preceding cases, this behaviour is probably triggered by the resonant energy transfer between the kinetic and internal degrees of freedom, that is, the bound modes or quasi-normal modes of the Q-ball. As we saw in Fig. 4, the Feshbach resonance is especially easily excited if the Q-ball is perturbed by the presence of another Q-ball. Hence, it may participate in the resonant energy transfer mechanism. In fact, the Feshbach resonances are known to play a significant role in kink dynamics [50]. This should be further studied.

Looking from a wider perspective, the oscillon origin of the charge-swapping once again underlines the very close relation between oscillons and Q-balls in complex field theories. In fact, as recently discovered, these objects are connected by an approximate duality [35]. Speaking precisely, an oscillon can be viewed as a bound state of Q-ball and anti-Q-ball, located on top of each opther. Consequently, the charge-swapping phenomenon may also find a dual description as a four-Q-ball state.

Acknowledgements

The authors acknowledge support from the Spanish Ministerio de Ciencia e Innovacion (MCIN) with funding from the European Union NextGenerationEU (Grant No. PRTRC17.I1) and the Consejeria de Educacion from JCyL through the QCAYLE project, as well as the grant PID2023-148409NB-I00 MTM. K. S. acknowledges financial support from the Polish National Science Centre (Grant No. NCN 2021/43/D/ST2/01122).

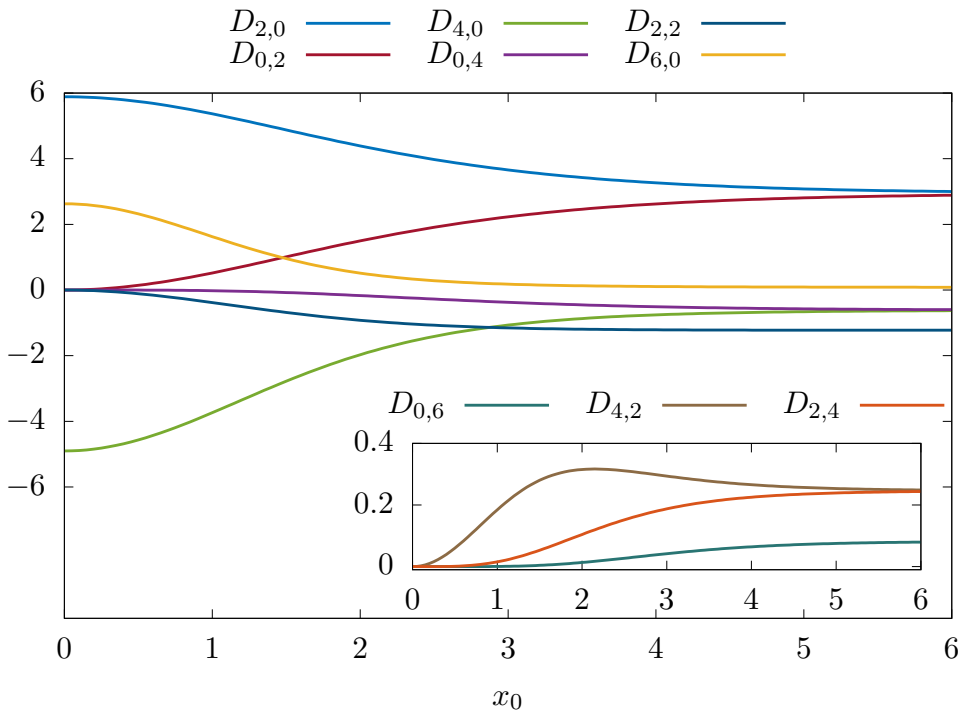

Figure 10. Dependence of the couplings in the effective potential on the position of the centres x_0.

A Effective potential

The coefficients in the potential of the CCM are related as follows

$$D_{2,0} = C_1^{(0)} + C_1^{(1)}, \quad D_{0,2} = C_1^{(0)} - C_1^{(1)}, \tag{A.1}$$

$$D_{4,0} = C_2^{(0)} + C_2^{(1)} + C_2^{(2)}, \quad D_{0,4} = C_2^{(0)} - C_2^{(1)} + C_2^{(2)}, \quad D_{2,2} = 2C_2^{(0)} - 6C_2^{(2)}, \tag{A.2}$$

$$D_{6,0} = C_3^{(0)} + C_3^{(1)} + C_3^{(2)} + C_3^{(3)}, \quad D_{0,6} = C_3^{(0)} - C_3^{(1)} + C_3^{(2)} - C_3^{(3)}, \tag{A.3}$$

$$D_{4,2} = 3C_3^{(0)} + C_3^{(1)} - 5C_3^{(2)} - 15C_3^{(3)}, D_{2,4} = 3C_3^{(0)} - C_3^{(1)} - 5C_3^{(2)} + 15C_3^{(3)}, \tag{A.4}$$

where the non-zero constants $C_k^{(j)}$ are given by the following formulas

$$C_1^{(0)} = \int dx \left(f'_\omega(x+x_0)^2 + f_\omega(x+x_0)^2\right) + \int dx \left(f'_\omega(x-x_0)^2 + f_\omega(x-x_0)^2\right), \tag{A.5}$$

$$C_2^{(0)} = -\int dx \left(f_\omega(x+x_0)^4 + f_\omega(x+x_0)^2 f_\omega(x-x_0)^2 + f_\omega(x-x_0)^4\right), \tag{A.6}$$

$$C_3^{(0)} = \beta \int dx \left(f_\omega(x+x_0)^6 + 9 f_\omega(x+x_0)^4 f_\omega(x-x_0)^2\right. \tag{A.7}$$

$$\left. +9 f_\omega(x+x_0)^2 f_\omega(x-x_0)^4 + f_\omega(x-x_0)^6\right), \tag{A.8}$$

$$C_1^{(1)} = \int dx \left(f'_\omega(x+x_0) f'_\omega(x-x_0) + f_\omega(x+x_0) f_\omega(x-x_0)\right), \tag{A.9}$$

$$C_2^{(1)} = -4 \int dx \left(f_\omega(x+x_0)^3 f_\omega(x-x_0) + f_\omega(x+x_0) f_\omega(x-x_0)^3\right), \tag{A.10}$$

$$C_3^{(1)} = 6\beta \int dx \left(f_\omega(x+x_0)^5 f_\omega(x-x_0)\right. \tag{A.11}$$

$$\left. +3 f_\omega(x+x_0)^3 f_\omega(x-x_0)^3 + f_\omega(x+x_0) f_\omega(x-x_0)^5\right), \tag{A.12}$$

$$C_2^{(2)} = -2 \int dx \left(f_\omega(x+x_0)^2 f_\omega(x-x_0)^2\right), \tag{A.13}$$

$$C_3^{(2)} = 6\beta \int dx \left(f_\omega(x+x_0)^4 f_\omega(x-x_0)^2 + f_\omega(x+x_0)^2 f_\omega(x-x_0)^4\right), \tag{A.14}$$

$$C_3^{(3)} = 2\beta \int dx \left(f_\omega(x+x_0)^3 f_\omega(x-x_0)^3\right). \tag{A.15}$$

$$\tag{A.16}$$

In the limit $x_0 \to \infty$, the potential $V(\alpha, \theta)$ becomes independent of θ, as only the terms proportional to $C_k^{(0)}$ remain non-zero:

$$V(\alpha) = \sum_{k=1}^{3} C_k^{(0)} \alpha^{2k} = C_1^{(0)} \alpha^2 + C_2^{(0)} \alpha^4 + C_3^{(0)} \alpha^6. \tag{A.17}$$

Therefore, the potential becomes axially symmetric in this limit.

By making the change to Cartesian coordinates, the new coefficients D can be written in terms of $C_k^{(0)}$:

$$D_{2,0} = D_{0,2} = C_1^{(0)} = 2 \int dx \left(f'_\omega(x)^2 + f_\omega(x)^2\right) , \tag{A.18}$$

$$D_{4,0} = D_{0,4} = \frac{1}{2} D_{2,2} = C_2^{(0)} = -2 \int dx \; f_\omega(x)^4 , \tag{A.19}$$

$$D_{6,0} = D_{0,6} = \frac{1}{3} D_{4,2} = \frac{1}{3} D_{2,4} = C_3^{(0)} = 2\beta \int dx \; f_\omega(x)^6. \tag{A.20}$$

In Fig. 10 we plot the dependence of the coefficients D on x_0. The asymptotic values of the parameters D at $x_0 \to \infty$ are

$$D_{2,0} = D_{0,2} = C_1^{(0)} = 2.94398 \tag{A.21}$$

$$D_{4,0} = D_{0,4} = \frac{1}{2} D_{2,2} = C_2^{(0)} = -0.612644 \tag{A.22}$$

$$D_{6,0} = D_{0,6} = \frac{1}{3} D_{4,2} = \frac{1}{3} D_{2,4} = C_3^{(0)} = 0.164228. \tag{A.23}$$

In Fig. 11, we show the effective potential in the variables X, Y.

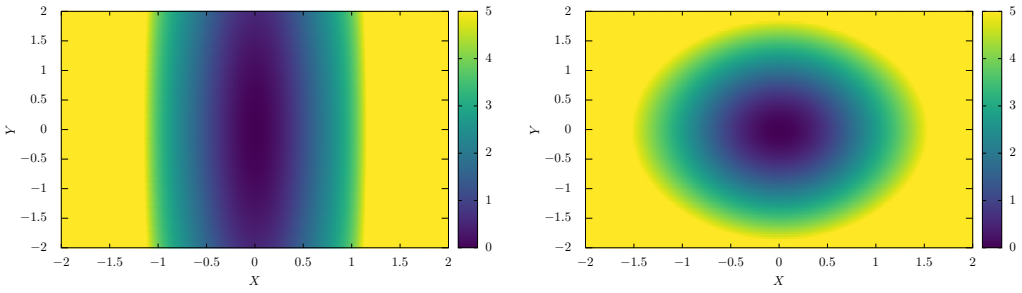

Figure 11. The effective potential V(X,Y) for $x_0 = 0.5$ (left) and $x_0 = 3$ (right).

References

[1] R. Friedberg, T. D. Lee and A. Sirlin, *A Class of Scalar-Field Soliton Solutions in Three Space Dimensions*, *Phys. Rev. D* **13** (1976) 2739–2761.

[2] S. R. Coleman, *Q-balls*, *Nucl. Phys. B* **262** (1985) 263.

[3] A. Kusenko and M. E. Shaposhnikov, *Supersymmetric Q balls as dark matter*, *Phys. Lett. B* **418** (1998) 46–54, [hep-ph/9709492].

[4] M. Dine and A. Kusenko, *The Origin of the matter - antimatter asymmetry*, *Rev. Mod. Phys.* **76** (2003) 1, [hep-ph/0303065].

[5] K. Enqvist and A. Mazumdar, *Cosmological consequences of MSSM flat directions*, *Phys. Rept.* **380** (2003) 99–234, [hep-ph/0209244].

[6] V. Cardoso and P. Pani, *Testing the nature of dark compact objects: a status report*, *Living Rev. Rel.* **22** (2019) 4, [1904.05363].

[7] D. J. Kaup, *Klein-gordon geon*, *Phys. Rev.* **172** (Aug, 1968) 1331–1342.

[8] R. Ruffini and S. Bonazzola, *Systems of self-gravitating particles in general relativity and the concept of an equation of state*, *Phys. Rev.* **187** (Nov, 1969) 1767–1783.

[9] S. L. Liebling and C. Palenzuela, *Dynamical boson stars*, *Living Rev. Rel.* **26** (2023) 1, [1202.5809].

[10] K. Enqvist and M. Laine, *Q-ball dynamics from atomic Bose-Einstein condensates*, *JCAP* **08** (2003) 003, [cond-mat/0304355].

[11] Y. M. Bunkov and G. E. Volovik, *Magnons condensation into Q-ball in He-3 - B*, *Phys. Rev. Lett.* **98** (2007) 265302, [cond-mat/0703183].

[12] R. Battye and P. Sutcliffe, *Q-ball dynamics*, *Nucl. Phys. B* **590** (2000) 329–363, [hep-th/0003252].

[13] P. Bowcock, D. Foster and P. Sutcliffe, *Q-balls, integrability and duality*, *Journal of Physics A: Mathematical and Theoretical* **42** (2009) 085403.

[14] M. Axenides, S. Komineas, L. Perivolaropoulos and M. Floratos, *Dynamics of nontopological solitons: Q balls*, *Phys. Rev. D* **61** (2000) 085006, [hep-ph/9910388].

[15] E. J. Copeland, P. M. Saffin and S.-Y. Zhou, *Charge-Swapping Q-balls*, *Phys. Rev. Lett.* **113** (2014) 231603, [1409.3232].

[16] Q.-X. Xie, P. M. Saffin and S.-Y. Zhou, *Charge-Swapping Q-balls and Their Lifetimes*, *JHEP* **07** (2021) 062, [2101.06988].

[17] S.-Y. Zhou, *Non-topological solitons and quasi-solitons*, 2411.16604.

[18] I. L. Bogolyubsky and V. G. Makhankov, *On the Pulsed Soliton Lifetime in Two Classical Relativistic Theory Models*, *JETP Lett.* **24** (1976) 12.

[19] M. Gleiser, *Pseudostable bubbles*, *Phys. Rev. D* **49** (1994) 2978–2981, [hep-ph/9308279].

[20] E. J. Copeland, M. Gleiser and H. R. Muller, *Oscillons: Resonant configurations during bubble collapse*, *Phys. Rev. D* **52** (1995) 1920–1933, [hep-ph/9503217].

[21] G. Fodor, P. Forgacs, Z. Horvath and M. Mezei, *Computation of the radiation amplitude of oscillons*, *Phys. Rev. D* **79** (2009) 065002, [0812.1919].

[22] G. Fodor, P. Forgacs, Z. Horvath and M. Mezei, *Radiation of scalar oscillons in 2 and 3 dimensions*, *Phys. Lett. B* **674** (2009) 319–324, [0903.0953].

[23] N. Graham and N. Stamatopoulos, *Unnatural Oscillon Lifetimes in an Expanding Background*, *Phys. Lett. B* **639** (2006) 541–545, [hep-th/0604134].

[24] P. Salmi and M. Hindmarsh, *Radiation and Relaxation of Oscillons*, *Phys. Rev. D* **85** (2012) 085033, [1201.1934].

[25] H.-Y. Zhang, M. A. Amin, E. J. Copeland, P. M. Saffin and K. D. Lozanov, *Classical Decay Rates of Oscillons*, *JCAP* **07** (2020) 055, [2004.01202].

[26] J. Olle, O. Pujolas and F. Rompineve, *Recipes for oscillon longevity*, *JCAP* **09** (2021) 015, [2012.13409].

[27] F. van Dissel, O. Pujolas and E. I. Sfakianakis, *Oscillon spectroscopy*, *JHEP* **07** (2023) 194, [2303.16072].

[28] M. Gleiser, N. Graham and N. Stamatopoulos, *Generation of Coherent Structures After Cosmic Inflation*, *Phys. Rev. D* **83** (2011) 096010, [1103.1911].

[29] M. A. Amin, R. Easther, H. Finkel, R. Flauger and M. P. Hertzberg, *Oscillons After Inflation*, *Phys. Rev. Lett.* **108** (2012) 241302, [1106.3335].

[30] S.-Y. Zhou, E. J. Copeland, R. Easther, H. Finkel, Z.-G. Mou and P. M. Saffin, *Gravitational Waves from Oscillon Preheating*, *JHEP* **10** (2013) 026, [1304.6094].

[31] J. Ollé, O. Pujolàs and F. Rompineve, *Oscillons and Dark Matter*, *JCAP* **02** (2020) 006, [1906.06352].

[32] J. C. Aurrekoetxea, K. Clough and F. Muia, *Oscillon formation during inflationary preheating with general relativity*, *Phys. Rev. D* **108** (2023) 023501, [2304.01673].

[33] D. Ciurla, P. Dorey, T. Romańczukiewicz and Y. Shnir, *Perturbations of Q-balls: from spectral structure to radiation pressure*, *JHEP* **07** (2024) 196, [2405.06591].

[34] F. Blaschke, T. Romańczukiewicz, K. Sławińska and A. Wereszczyński, *Oscillons from Q-balls through Renormalization*, *Phys. Rev. Lett.* **134** (2025) 081601, [2410.24109].

[35] F. Blaschke, T. Romanczukiewicz, K. Slawinska and A. Wereszczynski, *Q-ball polarization – a smooth path to oscillons*, 2502.20519.

[36] D. K. Campbell, J. F. Schonfeld and C. A. Wingate, *Resonance structure in kink-antikink interactions in φ 4 theory* , *Physica D* **9** (1983) 1.

[37] T. Sugiyama, *Kink-Antikink collisions in the two-dimensional phi**4 model*, *Prog. Theor. Phys.* **61** (1979) 1550–1563.

[38] N. S. Manton, K. Oles, T. Romanczukiewicz and A. Wereszczynski, *Collective Coordinate Model of Kink-Antikink Collisions in $\phi 4$ Theory*, *Phys. Rev. Lett.* **127** (2021) 071601, [2106.05153].

[39] I. Takyi and H. Weigel, *Collective Coordinates in One-Dimensional Soliton Models Revisited*, *Phys. Rev. D* **94** (2016) 085008, [1609.06833].

[40] F. C. Lima, F. C. Simas, K. Z. Nobrega and A. R. Gomes, *Scattering of metastable lumps in a model with a false vacuum*, *Phys. Lett. B* **822** (2021) 136707, [2108.13579].

[41] J. a. G. F. Campos and A. Mohammadi, *Wobbling double sine-Gordon kinks*, *JHEP* **09** (2021) 067, [2103.04908].

[42] S. Krusch, M. Rees and T. Winyard, *Scattering of vortices with excited normal modes*, *Phys. Rev. D* **110** (2024) 056050, [2406.04164].

[43] A. Alonso Izquierdo, N. S. Manton, J. Mateos Guilarte and A. Wereszczynski, *Collective coordinate models for 2-vortex shape mode dynamics*, *Phys. Rev. D* **110** (2024) 085006, [2405.20249].

[44] F. Blaschke, T. Romańczukiewicz, K. Sławińska and A. Wereszczyński, *Amplitude modulations and resonant decay of excited oscillons*, *Phys. Rev. E* **110** (2024) 014203, [2403.00443].

[45] N. S. Manton, *A Remark on the Scattering of BPS Monopoles*, *Phys. Lett. B* **110** (1982) 54–56.

[46] F. Blaschke, T. Romańczukiewicz, K. Sławińska and A. Wereszczyński, *Oscillons from Q-balls*, *Phys. Rev. D* **111** (2025) 036034, [2502.09136].

[47] N. S. Manton and T. Romańczukiewicz, *Simplest oscillon and its sphaleron*, *Phys. Rev. D* **107** (2023) 085012, [2301.09660].

[48] S. Navarro-Obregón, L. M. Nieto and J. M. Queiruga, *Inclusion of radiation in the collective coordinate method approach of the $\phi 4$ model*, *Phys. Rev. E* **108** (2023) 044216, [2305.00497].

[49] C. Adam, N. S. Manton, K. Oles, T. Romanczukiewicz and A. Wereszczynski, *Relativistic moduli space for kink collisions*, *Phys. Rev. D* **105** (2022) 065012, [2111.06790].

[50] A. García Martín-Caro, J. Queiruga and A. Wereszczynski, *Feshbach resonances and dynamics of BPS solitons*, 2501.02589.